Nationaal Lucht- en Ruimtevaartlaboratorium
National Aerospace Laboratory NLR

NLR TP 96320

Design and testing of a low self-noise aerodynamic microphone forebody

T. Dassen, H. Holthusen, and M. Beukema

DOCUMENT CONTROL SHEET

	ORIGINATOR'S REF.		SECURITY CLASS.
	NLR TP 96320 U		**Unclassified**

ORIGINATOR
National Aerospace Laboratory NLR, Amsterdam, The Netherlands

TITLE
Design and testing of a low self-noise aerodynamic microphone forebody

PREPARED FOR
The 2nd AIAA/CEAS Aeroacoustics Conference, May 6-8, 1996, State College, PA.

AUTHORS	DATE	pp	ref
T. Dassen, H. Holthusen and M. Beukema	**960514**	**15**	**14**

DESCRIPTORS

Acoustic impedance	**Nose cones**
Cavity resonators	**Screens**
Measuring instruments	**Self excitation**
Microphones	**Sound transducers**
Noise spectra	**Wind tunnel apparatus**

ABSTRACT
An extensive study on the origin and improvement of the self-noise characteristics of aerodynamic microphone forebodies (AMF) was carried out. Theoretical analysis of the pressure distribution and the boundary layer development along the outer surface of the forebody revealed that the position of the screen and the roughness height may be extremely critical. Based on this knowledge, an AMF with a more stable boundary layer at the screen position was developed. This AMF exhibited a better self-noise behaviour up to 80 m/s but only for small flow angles.
A further series of experiments with a modular AMF assembly showed that the geometrical details of the screen affect this behaviour, and led to the design of an AMF with a special perforated plate as a screen and a different number and geometry of the cavity holes. The flow resistance of this perforated plate was selected on its capability to subdue cavity shear flow oscillations over a wide angular range while the loss of sensitivity of the AMF is kept to a minimum. The influence on the free-field response of the improved AMF was determined in an anechoic facility.

Contents

1 Table
17 Figures

(15 pages in total)

This page is intentionally left blank.

DESIGN AND TESTING OF A LOW SELF-NOISE AERODYNAMIC MICROPHONE FOREBODY

Ton Dassen*
National Aerospace Laboratory NLR, Emmeloord, The Netherlands

Hermann Holthusen+
German-Dutch Wind Tunnel DNW, Emmeloord, The Netherlands

Martijn Beukema†
Twente University of Technology, The Netherlands

An extensive study on the origin and improvement of the self-noise characteristics of aerodynamic microphone forebodies (AMF) was carried out. Theoretical analysis of the pressure distribution and the boundary layer development along the outer surface of the forebody revealed that the position of the screen and the roughness height may be extremely critical. Based on this knowledge, an AMF with a more stable boundary layer at the screen position was developed. This AMF exhibited a better self-noise behaviour up to 80 m/s but only for small flow angles.
A further series of experiments with a modular AMF assembly showed that the geometrical details of the screen affect this behaviour, and led to the design of an AMF with a special perforated plate as a screen and a different number and geometry of the cavity holes. The flow resistance of this perforated plate was selected on its capability to subdue cavity shear flow oscillations over a wide angular range while the loss of sensitivity of the AMF is kept to a minimum. The influence on the free-field response of the improved AMF was determined in an anechoic facility.

Nomenclature

C_p = non-dimensional pressure
c_0 = speed of sound (m/s)
D = microphone outer diameter (m)
d = screen hole diameter (mm)
f = frequency (Hz)
H = cavity length (m)
k = wave number (1/m)
L = cavity hole diameter (m)
L_i = sound pressure response (dB)
l = distance between screen holes (mm)
M_s = mass reactance (m)
m = circumferential mode index (Eq. 7)
m = vortex shedding index (Eq. 5)
n = axial mode index
R = cavity radius (m)
R_s = non-dimensional resistance
r = radial co-ordinate (m)
U_0 = free flow velocity (m/s)
U_c = convective flow velocity (m/s)
U_τ = friction velocity (m/s)
v = local flow velocity (m/s)
x = axial co-ordinate (m)
Z = impedance (kg/m^2s^2)
z_{crit} = critical surface roughness (m)

α = angle of attack (deg)
δ = boundary layer thickness (m)
Δ_{FF} = free-field correction (dB)
Θ = axial sound incidence angle (deg)
θ = momentum loss thickness (m)
λ_v = vortex wavelength (m)
ξ = azimuthal angle (deg)
ρ = fluid density (kg/m^3)
μ = radial mode index
$\varepsilon_{m\mu}$ = modal eigenvalue

M = Mach number (U_0/c_0)
Re_θ = Reynolds number based on θ ($U_0\theta/\nu$)
Re_D = Reynolds number based on D (U_0D/ν)
St = Strouhal number (fd/U_0 in Eq. 4 or fL/U_0 in Fig. 12)

Introduction

Since the foundation of the German-Dutch Wind Tunnel (DNW) in 1979, many acoustic studies have been carried out in the 8×6 m^2 open jet of this anechoic facility. In the past, B&K 1/4" 4135 or 1/2" 4133 microphones equipped with

*Research engineer
+Research engineer
†Student

B&K UA 0385 and UA 0386 aerodynamic forebodies (indicated as 'nose cones' in the B&K handbooks) were used when measurements in the flow were performed. The problem of the disturbing self-noise peaks of these nose cones became apparent firstly in 1985 when in-flow measurements of the airframe noise of a 1/11th scale model of a Boeing aircraft were carried out (Ref. 1).
With the purpose to analyze and understand the peaky self-noise behaviour, an experimental study in the 1:10 DNW pilot-tunnel was commenced in 1990. These tests showed that the self-noise characteristics of the B&K microphones is of almost random nature, impeding any proper correction. With the aim to design a nose cone with low self-noise characteristics, a number of activities was then initiated, comprising analyses of the boundary layer stability, a qualitative study on the 'edge tone phenomena', and a large series of experiments, among other things using a 1/4" and a 1" modular assembly of an AMF.

Aerodynamic Microphone Forebodies

In the case of measurements in air flow of high speed and well defined direction, Aerodynamic Microphone Forebodies (AMFs) are recommended as a substitute to the microphone protection grid or wind screen which is normally applied at low wind speeds (< 20 m/s). These AMFs are intended to minimize the pressure fluctuations at the microphone membrane which are caused by the convection or impingement of turbulence in the flow or boundary layer past the microphone outer surface.

B&K 'Nose Cones'

Brüel & Kjær (B&K) equipment is used for acoustic testing in the DNW, as it is designed for accurate sound measuring purposes and complies with international standards on sound measurements.
The standard Brüel & Kjær (B&K) 'nose cones' UA 0355, UA 0385, UA 0386 and UA 0387 can be connected to the 1/8", 1/4", 1/2" and 1" microphone cartridges. It is described in Ref. 2 that its streamlined shape is designed to give the least possible resistance to air flow, thereby reducing the turbulence. A fine wire mesh around the AMF permits sound pressure transmission to the microphone diaphragm (see Fig. 1).

B&K AMF Self-noise Levels

Self-noise spectra of the B&K microphones equipped with B&K AMFs are presented in Ref. 2 for flow speeds up to 160 km/h (44.5 m/s) and for frequencies up to 20 kHz. For these flow speeds and frequency range, all AMF configurations yield acceptable self-noise spectra, i.e. exhibit a limited number of peaks only in the case of the smallest (1/4" and 1/8") configurations.
The self-noise problem of B&K AMFs became apparent after a series of acoustic in-flow measurements on a 1:11 scale model of a Boeing aircraft in the German-Dutch Wind Tunnel at flow speeds ranging from 60 m/s up to 80 m/s (Ref. 1). Here, ultrasonic frequencies had to be measured in order to enable the correction of measured data to their full-scale equivalent. Comparison of the 1/3octave band out-of-flow and in-flow measurements revealed AMF self-noise tones for frequencies above 16 kHz (see Fig. 3).

Further narrowband analysis showed that each individual AMF had its own 'peculiar' set of tones and that the tones changed not only with flow speed but also with angle of attack. Peaks, once apparent, were found to 'switch' quite easily between several preference frequencies and appeared and disappeared without a clear cause. Their onset obviously depended on the quality of the flow and/or the presence of other noise sources. In spite of numerous attempts to get consistent data by proper cleaning and handling, these phenomena remained.

Flow Analysis and AMF Outer Shape

The character of self-noise as pictured in the previous section indicates local, unsteady flow phenomena close to the wire mesh. Boundary-layer instabilities, transition or even flow separation will cause high levels of hydrodynamic pressure fluctuations which will be sensed by the nearby microphone membrane. In the case of the relatively low Reynolds number (Re_D<1.5×10^5), which occur in the case of low-Mach number (M<0.25) flow around a one inch microphone, transition is mainly influenced by the local pressure gradient along the microphone AMF outer surface, but can also be enforced by surface roughness, for example by irregularities present at the position of the wire mesh, or by reverse flow through the wire mesh due to an axial pressure gradient at the position of this wire mesh. Transition can even be caused by an acoustic wave field.
In the next sections it is explained how pressure distributions and boundary layer characteristics of several existing AMFs were investigated and how this led to the design of a new AMF outer shape. This series of AMFs comprised the B&K AMF, an AMF designed and used by the Delft University of Technology (TUD AMF) and very much resembling the Prandtl-tube shape, and an AMF having an ellipsoidal shape (with 1:6 axis lengths ratio). The outer shapes of these AMFs are presented in Fig. 4.

Pressure Distributions

The potential flow about and the pressure distributions along the outer surface of axially symmetric bodies were calculated using a panel method. The results of these calculations on the aforementioned AMF shapes and the positions of the screens are shown in Fig. 5.

Boundary-layer behaviour

The pressure distributions were further used to calculate the envelopes of the boundary layer momentum thickness (θ), the Reynolds number based on the momentum thickness ($Re_\theta=U_0\theta/\upsilon$), and the friction velocity (U_τ) as well as the profiles of the velocity in the boundary layer at the screen positions. For this, a laminar axi-symmetric version of the NLR BOLA finite difference method, developed by Lindhout was used. (Ref. 3).
Re_θ can be used to estimate whether transition will occur. In general, it can be assumed that Re_θ=320 will be a lower limit for fully developed turbulent boundary layers. Smaller values indicate that transition will only occur as a result of local irregularities on the surface. On the other hand, Re_θ and U_τ can be used to estimate the critical surface roughness, z_{crit}. All boundary layer calculations were conducted with Re_D=6×10^4 which, in case of a 1/4" diameter AMF, implies a (free) flow velocity of 66.5 m/s.

In the case of laminar flow, the proportionalities

$$\theta \propto Re_D^{-1/2} \quad (1)$$

$$Re_\theta \propto Re_D^{-1/2} \quad (2)$$

and

$$U_\tau \propto Re_D^{3/4} \quad (3)$$

can be used to obtain θ, Re_θ and U_τ for other values of Re_D (eg. Ref. 13). The envelopes of θ, Re_θ, U_τ and z_{crit} are presented in Fig. 6a-d. The boundary layer velocity profiles are shown in Fig. 7.

B&K AMF

The pressure distribution of the B&K AMF shows to have the lowest value relatively far downstream, and a significant axial pressure gradient is still present at screen position which is felt to be unfavourable with respect to flow through the screen.
The value of θ is relatively small due to the short trajectory with an unfavourable pressure gradient. The value increases rapidly at the beginning of the screen, due to the unfavourable pressure gradient at this position. Here, Re_θ remains significantly smaller than 320, indicating that the boundary layer will keep its laminar character unless a flow disturbance occurs (i.e. reverse flow through the screen). The value of U_τ is relatively large shortly behind the nose, while its value decreases rapidly close to the screen, leading to a point of inflexion in the boundary layer velocity profile, indicating that the flow is close to separation. The value of z_{crit} is the smallest of all.

TUD AMF

The pressure distribution of the TUD AMF reveals a large underpressure just downstream of the nose of the AMF, which makes it sensitive to flow separation at angles of attack. Further downstream, the pressure attains the level of undisturbed pressure rather smoothly, apparently keeping a constant margin with respect to laminar separation. This is clearly shown by the smooth envelope of U_τ downstream of the point of the lowest pressure.
The value of θ is relatively large due to the long trajectory of an unfavourable pressure gradient. As a result, Re_θ has a relatively high value at the position of the screen, but is still smaller than 320 indicating that the boundary layer will be laminar. The value of z_{crit} exceeds the value for the B&K AMF by some 30%, mainly as a result of the boundary layer being thicker. The boundary layer velocity profile exhibits no inflexion point due to the absence of a significant pressure gradient at the position of the screen.

Ellipsoidal AMF

The ellipsoidal AMF exhibits a fairly flat pressure distribution and needs relatively much length to attain the undisturbed pressure. Its screen is positioned in a region where a small pressure gradient is still present. The value of θ is relatively small due to the fact that the trajectory with an unfavourable pressure gradient is rather short. The boundary layer will be laminar as a result of Re_θ remaining smaller than 320 even downstream of the screen. U_τ decreases very gradually, meaning that there is no tendency of the flow to separate. The boundary layer velocity profile, however, exhibits an inflexion point, indicating that the boundary layer will be unstable. The value of z_{crit} is relatively small.

Design of a New AMF Outer Shape

The NLR panel method used for the calculation of streamlines and pressure distributions in potential flows allows for the inclusion of sources and/or sinks. This feature enables the design of a new AMF shape since this shape follows from the condition of fully tangential flow along the surface, i.e. the surface contour coincides with a streamline. Hence, the source distribution can be varied while the streamlines and the associated pressure distribution can be calculated (for more details see Ref. 4 and Ref. 5).
The design of a new AMF outer shape was focussed on a zero pressure gradient at screen position without a far downstream position of the screen ($Re_\theta < 320$) and while avoiding very low values of underpressure just downstream of the nose. This latter is expected to make the boundary layer very sensitive to separation in case of angle of attack.

The new 'NLR-DNW' AMF is shown in Fig. 8. Its shape is 'in between' the TUD and the ellipsoidal shapes. The pressure distribution (see Fig. 5) shows a relatively small underpressure rather shortly downstream of the nose and attains, very gradually, the undisturbed pressure, approximately four head diameters downstream of the nose.
The value of θ is relatively large due to the long trajectory with an unfavourable pressure gradient. Re_θ at screen position is (slightly) smaller than 320. The envelope of U_τ and the absence of an inflexion point in the boundary layer velocity profile indicate that there is no tendency towards boundary layer instability or separation. The value of z_{crit} is approximately the same as for the TUD AMF (Fig. 6a-d and Fig. 7).

Performance of NLR-DNW AMF

The performance of the NLR-DNW AMF was investigated and compared to the B&K AMF in a first series of acoustic measurements in the open jet configuration of the 1:10 scale pilot tunnel of DNW. For this, a 1/4" and a 1/2" NLR-DNW AMF having the shape described in the previous section, were manufactured and mounted to 1/4" and 1/2" B&K microphone cartridges. Additionally, a dummy 1½" configuration with B&K and NLR-DNW AMFs was manufactured for flow visualisation purposes.

The flow visualisation studies using dye were performed at velocities between 10 m/s and 40 m/s in order to achieve Reynolds numbers comparable to these during measurement with 1/4" and 1/2" configurations. On both the B&K and the NLR-DNW AMF clear traces having a very regular pattern of black and white indicative for the accumulation and absence of dye were found. A picture of such a pattern is shown in Fig. 9. These patterns were found to exist only downstream of the upstream edge of the screen ring. For the B&K AMF this pattern appeared at a basically lower velocity than for the NLR model. The exact lower limits were hard to assess due to relatively short time available for the dye to settle. Several further tests, among others after a roughness strip was attached to the AMFs upstream of the screen revealed that the flow at the screen position is essentially laminar and the patterns are caused by instability waves in the boundary layer initiated by the upstream edge of the screen.

The results of the acoustic measurements on the B&K AMFs confirmed the formerly observed unpredictable and peaky self-noise behaviour.
The NLR-DNW AMF was found to exhibit a very consistent self-noise behaviour. However, one strong, velocity dependent tone was found to develop around 16 kHz at 80 m/s. In case the AMF was set at an angle of attack, this peak showed to increase in amplitude as well as in frequency and was even found to contain more energy than the self-noise peaks of the B&K AMF. Self-noise spectra of the B&K and NLR-DNW AMFs are given as a function of flow velocity and angle of attack in Fig. 10a-b and Fig 11a-b.

The general impression resulting from the measurements on the 1/2" configurations is that these AMFs are slightly less susceptible to self-noise peaks than the 1/4" configurations. A possible explanation might be that since the same screen material is used, the sensitivity to transition is less, i.e. the allowable roughness height is larger.

Investigation of Unsteady Flow Phenomena

A further study on the reduction of self-noise peaks in the case of angle of attack was aimed at cavity shear flow oscillations which may result from i) the inherently unstable flow past the cavity or ii) coupled vortex shedding at the upstream edge of the individual screen holes.
These phenomena and the findings of a series of experiments using a modular AMF assembly are described in the next sections.

Flow-Induced Resonance of Screen-Covered Cavities

In Ref. 6 it is described how strong acoustic resonances are created in case vortices, shed from the screen holes, are coupled with cavity pressure oscillations. Here, the coupling takes place by a matched propagation of vortices which induce in-phase velocities at the next (downstream) orifices. These in-phase velocities excite cavity acoustic pressure resonance at cavity "room" modes. As airspeed is increased, the frequency of vortex shedding will increase and acoustic energy in the dominant cavity mode will decrease, while the energy in the higher mode(s) increases. The acoustic pressures radiate to the far field as tones.
The criterion for resonance or non-resonance is formulated in terms of a phase coupling parameter, which is equal to the ratio of vortex wavelength-to-hole spacing (λ_v/l with λ_v equal to the convection velocity U_c divided by the vortex shedding frequency f_v). Resonance will occur when that parameter is equal to 0.25, 0.5 or 1.0.
Using the natural shedding rate of the vortex street on the screen, f_v

$$f_v = \frac{St \times U_0}{d} \tag{4}$$

with St the Strouhal number, U_0 the free flow velocity and d the cavity screen hole diameter, and assuming that the vortex shedding rate must correspond to a cavity modal frequency f_c which was empirically determined to fulfil

$$f_v = (-0.01 + 0.10d)m\frac{U_c}{d} \qquad with\ m = 1,2,3,... \tag{5}$$

leads to

$$\frac{\lambda_v}{l} = \frac{U_c \frac{d}{l}}{U_0 m(-0.01 + 0.10d)} \tag{6}$$

for the phase coupling parameter.
Eq. 6 shows that λ_v/l is only a function of the hole diameter and spacing, i.e. a certain screen resonates or not independent of the flow speed (assuming that U_c/U_0 is independent from flow speed).
The frequencies of cylindrical cavity room resonances result from the solution of the Helmholtz equation describing the sound field in a closed hard-walled circular duct (eg. Ref. 7), and can be calculated using

$$f = \frac{c_0}{2}\left\{\frac{\varepsilon_{m\mu}}{\pi R} + \frac{n}{H}\right\} \tag{7}$$

with H the length of the cavity, R the radius of the cavity, $\varepsilon_{m\mu}$ the modal eigenvalue, m, n and μ the circumferential, axial and radial mode indices.

Oscillations of Flow Past Cavities

Shear layer oscillations have been the object of a large number of theoretical and experimental investigations (see eg. the list of references of Ref. 8 through 10).
Self-sustained shear layer oscillations may result from the unstable shear layer solely by interaction with the downstream cavity edge and by reacting on the boundary conditions at the upstream edge. This feedback loop may exist without cavity resonances or fluid-elastic coupling with the motion of a solid boundary (eg. a piston in the cavity). It occurs if the ratio of the cavity length to the acoustic wavelength is small, implying that the feedback takes place in the near-field of the acoustic source. The mechanism can therefore be regarded as essentially hydrodynamic. Non-resonant shear layer oscillation is a relatively low-amplitude phenomenon, i.e. is very inefficiently radiated into the far-field despite the fact that reasonably high levels of hydrodynamic pressure in the cavity occur.
This type of oscillation has some features in common with so-called 'edge tones', involving impingement of an oscillating free jet upon an edge (eg. Ref. 10). The onset of oscillations is expected to be attributable to disturbance growth in the shear layer, i.e. must undergo a minimum integrated amplification between separation and impingement. Hence, the presence of a cavity screen, damping the growth of shear layer oscillations or, depending on the flow resistance of the screen, even preventing the shear layer to become unstable may reduce of may even completely cancel the oscillations. Unfortunately, clear criteria for the onset or damping of oscillations have not been found in literature.
The frequency of cavity shear layer oscillation is expressed in terms of a Strouhal number based on the impingement length ($St=fL/U_0$). Variations of the Strouhal number with dimensionless length (L/δ) are presented in Ref. 9 and shown in Fig. 12 for laminar boundary layers at the upstream edge. These Strouhal number plots exhibit several stages which are reported to reveal a hysteresis behaviour i.e. depend on whether the cavity width or the velocity is being increased or decreased.

Theoretical Analysis

The expressions found in literature for the occurrence of resonant screen hole vortex shedding (Eq. 4 through 7) and the data on self-sustained cavity oscillations (Fig. 12) were used to estimate whether self-noise peaks had to be expected and if so, for which frequencies.
With screen holes diameters (d) of the order of 0.2 mm and holes distances (l) of 0.3 mm (35 % open), and U_c=0.5U_0, a value of 33 for the phase coupling parameter results (m=1), and does thus not fulfil the resonance condition unless m equals 33, 66 or 132. Since strong resonances were only reported for m=1 and weak resonances for m=2 and m=3 (Ref. 6), it may be concluded that resonant screen hole vortex shedding will not occur. This conclusion is further supported by the finding that cavity resonance frequencies are significantly higher than practically observed. Cavity mode resonance frequencies for the 1/4" AMF are listed up to 100 kHz in Table 1 using Eq. 7.

Taking the behaviour shown in Fig. 12 as a starting point, cavity shear layer oscillations seem to be more likely to occur. Unfortunately, the ranges for L/δ and fL/U_0 (St) presented in this figure, do not cover the values of these ratio's resulting from the measurements. At 3 degrees, where a tone starts to develop around 20 kHz, the boundary layer thickness δ at screen position is estimated to be a few tens of a millimetre, yielding a Reynolds number based on the boundary layer thickness, of the order of 1000 (U_0=80 m/s) and a value of the order of 25 for the ratio of hole diameter and boundary layer thickness. In case the stages of tones may be extrapolated to L/δ=25 a Strouhal number of 15 to 20 results, giving frequencies of a few hundreds of kHzs. Since the peak tones where observed at frequencies an order of magnitude smaller, it remains uncertain whether cavity shear layer oscillations play a role.

Modular AMF Assembly and Test Programme

Additionally, a series of experiments was performed to find out whether the shear layer oscillations are the cause of the AMF self-noise peaks or not. Therefore, a 1/4" and a 1" modular AMF assembly with the new outer shape and consisting of different extension rings, screen rings, microphone holders and internal (filler) plugs were manufactured and the various configurations were tested in the 1:10 scale pilot tunnel of DNW. The configurations were measured for flow speeds ranging from 10 m/s up to 90 m/s, and for flow angles ranging from 0 degrees up to 10 degrees. The microphones were placed on a low self-noise support and an extra microphone was placed out of the flow to detect whistling tones radiated from the AMF or its support.

Essentially two types experiments were performed:
I) Measurement of self-noise while varying the cavity volume and geometry.
II) Measurements of self-noise in case of angle of attack and while varying the azimuthal incidence angle.
The latter test was done as a result of the expectation that the positions of the cavity holes will be of influence on shear layer oscillations.
Analysis of a large number of data led to the following summary of the results:

i) The frequency of self-noise peaks was found to be only marginally dependent on the cavity volume and geometry.
ii) The far-field microphone did not record any of the tones appearing in the self-noise spectra.
iii) The occurrence and disappearance of tones was found to exhibit hysteresis (with respect to change in flow velocity as well as in angle of attack).
iv) Some tones were found to increase in frequency in case of increase of angle of attack, others were found to decrease in frequency.
v) In the case of angle of attack, self-noise spectra were found to depend on the azimuthal orientation of the AMF.

Analysis of Experimental Results

The findings as described in points i) through iii) very much indicate the presence of the 'edge-tone' phenomenon (i.e. cavity shear layer oscillations) and do not give any hints for the occurrence of acoustic cavity resonances coupled with matched vortex shedding at the screen holes. The finding that AMF self-noise peaks result from cavity edge-tones was also concluded from previous investigations on AMF self-noise behaviour at NASA (Ref. 11 and 12).

The phenomena as mentioned under points iv) and v) were further analyzed and were found to be strongly linked.
In the case of angle of attack, it can be easily derived that the potential flow velocity just outside the boundary layer flow can be described according to:

$$U(\alpha,\xi) = U_0\sqrt{\cos^2(\alpha) + 4\sin^2(\alpha)\sin^2(\xi)} \qquad (8)$$

with α the angle of incidence and ξ the microphone azimuthal angle (orientation with respect to the flow stagnation line). Depending on incidence angle and orientation of the holes with respect to the stagnation line significant differences in the effective flow velocity (up to a factor of 1.5 for most practical angles) and inherently the oscillation frequencies, can be expected. Consequently, the frequencies will follow Eq. 8. Hence, the frequencies can be seen to increase in case a hole is orientated at 'some distance' from the stagnation line (i.e. at an azimuthal angle larger than 30 deg.) or decrease in case a hole is orientated 'close to' the stagnation line (i.e. at an azimuthal angle smaller than 30 deg.) In practice, these phenomena were seen to occur but could not be linked to the AMF orientation in a quantitative way, most probably due to the fact that the dominant tones could not be correlated with the oscillation of one definite hole.

Adjustment of Screen and Hole Design

Assuming that cavity shear layer oscillations are the cause of the self-noise peaks, several measures to reduce these oscillations were investigated. As mentioned previously, oscillations can be subdued or even completely prevented by increasing the (flow) resistance of the screen. For this several materials were investigated, of course only after it was assured that these materials didn't exhibit the 'whistling' behaviour previously described as flow-induced resonances of screen-covered cavities.
Perforated plates were found to comply with the criterion of the critical surface roughness, but have the disadvantage of a non-linear behaviour with respect to flow velocity and amplitude of incident sound. Therefore, a special material, patented under the name PERFOLIN®, and manufactured by

STORK VECO B.V. The Netherlands was investigated. This material has horn-shaped orifices and has an excellent linear behaviour. A picture of a B&K wire-mesh and a PERFOLIN® perforated screen is given as Fig. 13.
With the screen impedance given by

$$Z/\rho c_0 = R_s + iM_s k \qquad (9)$$

with R_s the (non-dimensional) resistance and $M_s \times k$ the (non-dimensional) product of mass reactance and wave number, the resistance can be as low as 0.25. The mass reactance approximately equals 0.003 m which implies that the high-frequency loss of sensitivity of the AMF has to be accounted for (see next section).
After the geometry and number of the underlying cavity holes were adjusted (for reasons also explained in the next section) several PERFOLIN® screens (ranging from 46% open and 0.35 mm holes to 32% open and 0.2 mm holes) were tested in the 1:10 pilot tunnel of DNW.

Performance of Modified NLR-DNW AMF

The screen with a porosity of 32% and hole diameters of 0.2 mm was found to exhibit a significant improved self-noise behaviour, i.e. no significant peaks occurred for wind speeds up to 70 m/s and flow angles up to 10 degrees. This performance was established during a series of measurements on a real model in the open jet of the DNW, but was later found to depend on the quality of the tunnel flow. In the Small Anechoic Wind Tunnel (KAT) of NLR with a turbulence intensity level, v'/U_0, which is typically a few percents, i.e. two orders of magnitude higher than the DNW turbulence level, a significant peak was found to develop at a flow speed of 60 m/s. The frequency of this peak increases slightly with angle of attack. The self-noise spectra of the modified NLR-DNW AMF as measured in the KAT are given in Fig. 14. The spectra clearly exhibit much higher levels of broadband noise due to the relatively high turbulence levels of this tunnel.

Free-field Responses and Cavity Design

Determination of Free-field Corrections

The difference between the sensitivity of the microphone to the pressure actually existing at its diaphragm (the pressure response, $L_{P,c}(\Theta)$) and the sensitivity of the microphone to the pressure which would exist at that place in case the microphone would be absent (free-field response, L_{FF}) is called the free-field correction ($\Delta_{FF}(\Theta)$), and is normally expressed in decibels (dB). The free-field response in fact accounts for the sound diffraction by the geometry and the damping by the screen, depending on the incidence of the sound, and the impedance of the screen respectively.
Free-field responses of individual microphones equipped with an AMF, wind screen or protection grid can be determined in an anechoic facility of NLR. The set-up consists of a remote-controlled rotatable boom to which a microphone can be mounted, an acoustic source, and a fixed boom with a reference microphone to correct for variation in source level. To determine Δ_{FF} as a function of axial sound incidence angle, the microphone is rotated over 360 degrees while keeping the middle of the microphone diaphragm at exactly the same position.
Only after it was realized that the way the holes were positioned with respect to the direction of the sound could be of influence, azimuthal rotations were made and free-field corrections were determined. The results are given in Fig. 15 for 100 kHz for the 1/4" B&K AMF, clearly showing a pattern with six holes, implying a significant influence of the azimuthal sound incidence angle on the response. Further investigations revealed significant differences (up to 20 dB at 100 kHz) between individual B&K AMFs, due to the difference in hole and inner geometry.

Holes

The number of holes was increased from six to ten as a result of the finding that the free-field corrections strongly depend on the azimuthal orientation of the AMF. Initially mainly for structural reasons, 3 mm long and 1.1 mm wide slots instead of circular holes were made in the modified NLR-DNW AMF. The slot geometry is exactly equally open (approx. 30 mm^2) as the 6 hole geometry. The smaller width of the slots (as compared to the diameter of the circular holes) proved to have an additional favourable influence on the cancellation of tones in the case of angle of attack. This influence is expected to result from the decrease of the shear layer length in circumferential direction.
The dependency of free-field corrections on the azimuthal orientation is presented in Fig. 15 showing a significant improvement with respect to six hole configuration.

Cavity

In order to obtain AMFs yielding responses as consistent as possible, a series of 8 NLR-DNW AMFs was manufactured using computer-aided design and numerical grinding machines. Although the spreading in free-field responses showed to be much less, significant differences (up to 10 dB at 100 kHz) between individual AMFs were still established. The interior of the modified NLR-DNW AMF is shown in Fig. 16

Free-field Response of Modified NLR-DNW AMF

The (absolute) free-field corrections of the modified NLR-DNW AMF with 32% open PERFOLIN® are compared to the B&K AMF in Fig. 17 for two axial sound incidence angles (Θ), showing a loss of sensitivity of up to approximately 10 dB in the 30 to 70 kHz range.
The cavity resonance peak is shifted down from 30 kHz to 23 kHz which is exactly the frequency of the tone which starts to develop at flow speeds above 70 m/s. This may indicate that the cavity shear layer oscillations are indeed damped sufficiently, and that the 'tones' are now being caused by the amplification of the hydrodynamic disturbances which result from the convection of turbulence present in the KAT flow. The (relatively small) dependency of peak frequency on flow angle may in this case be explained by the known influence of boundary layer characteristics on the impedance of resonant cavities (Ref. 14). However, it has to be noted that no comprehensive analysis of these phenomena was made.

Results and Future Research

As a result of an extensive series of theoretical and experimental investigations on the boundary layer flow and self-noise behaviour of several AMF configurations, an improved AMF has been developed.

When used in the low-turbulent flow of the DNW, this improved AMF shows a consistent and predictable self-noise behaviour and exhibits no peaks up to flow speeds of approximately 70 m/s and flow angles of 10 degrees in the frequency range up to 60 kHz. At higher wind speeds self-noise tones start to develop, but contain significantly less energy compared to the self-noise tones of existing AMFs. However, the self-noise behaviour is observed to depend on the quality of the flow and will develop tones at a significant lower wind speed (60 m/s) and flow angle (close to zero degrees) in case the turbulence level of the flow is significantly higher than the turbulence level of the undisturbed DNW flow.
The improvements were obtained mainly by a new outer shape, the selection of a special type of a perforated plate as a cavity screen, and after modification of the number and geometry of the cavity holes and the interior.
The fact that free-field responses differ for every individual AMF has been investigated and reduced. However, significant differences in free-field responses are still observed, meaning that the modified NLR-DNW AMFs still require individual calibration.

In future, it will be tried to analyze and reduce the self-noise which develops at flow speeds above 70 m/s. Research on this topic will focus on the observed dependency of the peak levels on the quality of the flow, and, additionally, on the reduction of the amplification of the hydrodynamic disturbances by the cavity. This may be tried by further modification of the holes and cavity interior.
In conjunction with this, it has to be noted that broadband noise resulting from turbulence has only been marginally addressed thus far. Broadband noise levels, although orders of magnitudes below the initial peak noise levels, may become important in case in-flow measurements of relatively low levels of broadband airframe noise have to be performed. For this, a further study on the possible limitations imposed by AMF broadband self-noise levels is recommended.

Acknowledgement

The fruitful discussions on the AMF self-noise behaviour with Mr. Erling Frederiksen of Brüel & Kjær Denmark are greatfully acknowledged. The authors are also indebted to STORK VECO B.V. for the samples of PERFOLIN® made available to NLR for this research.
Last but not least, the authors would like to thank Mr. J.C.A. van Ditshuizen, currently at the European Transonic Wind Tunnel ETW, for his early initiatives to start the described research and Mr. A. de Bruin of the Department of Experimental Aerodynamics of NLR for his contributions to the analysis of the AMF boundary layer flow.

References

1Glover Jr., B.M., Shivashankara, B.N., *Aeroacoustic Testing in Wind Tunnels*, AIAA-paper 86-1986, 1986

[2]*Condenser Microphones and Microphone Preamplifiers for acoustic measurements*, B&K Data Handbook, 1982

[3]Lindhout, J.P.F., Moek, G., Boer, E., v.d. Berg, B., *A method for the calculation of 3D boundary layers on practical wing configurations*, Transactions of the ASME, March 1981, also NLR Technical Report 79003 U

[4]Dominicus, J., *A theoretical analysis of the self-noise problem based on calculations of the pressure distributions and boundary layer characteristics of various microphone configurations (in Dutch)*, Graduate report, Haarlem Polytechnic (NL), 1989

[5]van Ditshuizen, J.C.A., *Microphone Nose Cone Selfnoise, Results and Analysis of a Series of Consecutive Tests Regarding Selfnoise Behaviour of Different Types of Nose Cones*, DNW Technical Report 93-46, 1993

[6]Soderman, P.T., *Flow-Induced Resonance of Screen-Covered Cavities*, NASA Technical Paper 3052, 1990

[7]Munjal, M.L., *Acoustics of Ducts and Mufflers*, John Wiley and Sons, Inc., 1987, New York

[8]Rockwell, D., Naudascher, E., *Review-Self-Sustained Oscillations of Impinging Free Shear Layers*, Transactions of the ASME, vol. 100, 1978, pp. 152-165

[9]Rockwell, D., Naudascher, E., *Self-Sustained Oscillations of Impinging Free Shear Layers*, Ann. Rev. Fluid Mech., 1979, 11, pp. 67-94

[10]Karamcheti, K., Bauer, A.B., Shields, W.L., Stegen, G.R., Woolley, J.P., *Some Features of an Edge-Tone Field*, NASA Spec. Publ., 207, pp. 275-304, 1969

[11]Allen, C.S., Soderman, P.T., *Aeroacoustic Probe Design for Microphone to Reduce Flow-Induced Self-Noise*, AIAA-paper 93-4343, 1993

[12]Allen, C.S.,
Vandra, K., *Microphone Corrections for Accurate In-Flow Acoustic Measurements at High Frequency* , CEAS/AIAA paper 95-150, 1995

[13]Schlichting, H., *Boundary-Layer Theory*, Seventh Edition, McGraw-Hill, 1979, New York

[14]Kooi, J.W., Sarin, S.L., *An Experimental Study of the Acoustic Impedance of Helmholtz Resonator Arrays Under a Turbulent Boundary Layer*, AIAA-paper 81-1998, 1981

Table 1: Cavity room modes of 1/4" configuration up to 100 kHz (cavity inner radius=3 mm, cavity length=5 mm, c_0=340 m/s; from Eq. 7)

f (Hz)	m	μ	n	$\varepsilon_{m\mu}$
0	0	1	0	0
33189	1	1	0	1.84
34000	0	1	1	0
55015	2	1	0	3.05
67189	1	1	1	1.84
68000	0	1	2	0
69084	0	2	0	3.83
89015	2	1	1	3.05
96140	1	2	0	5.33

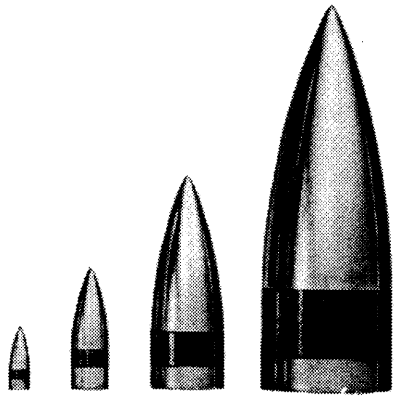

Fig.1: B&K Aerodynamic Microphone Forebodies UA 0355, UA 0385, UA 0386 and UA 0387 (from Ref. 2)

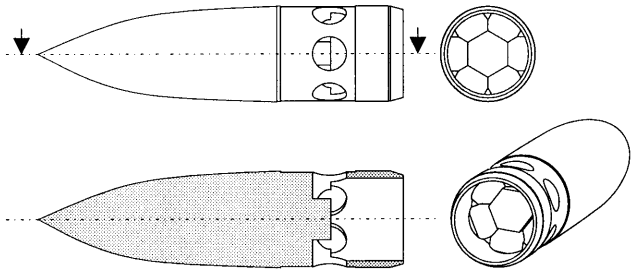

Fig.2: B&K AMF outer shape, cross section and interior

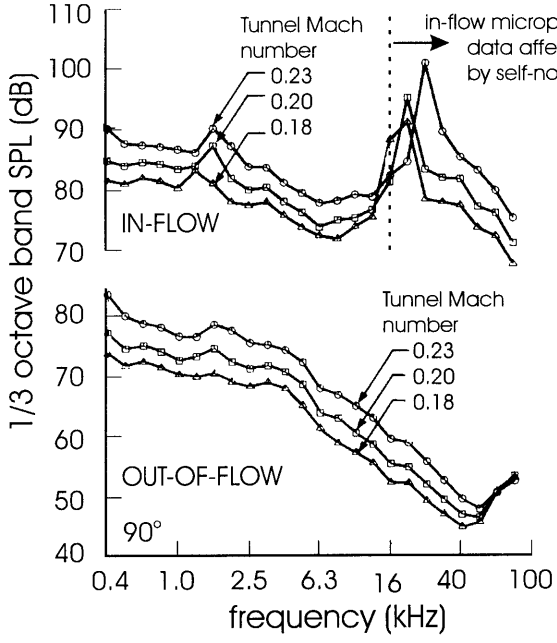

Fig.3: DNW 1/3octave band tunnel background noise levels showing in-flow microphone data affected by self-noise (after Ref. 1)

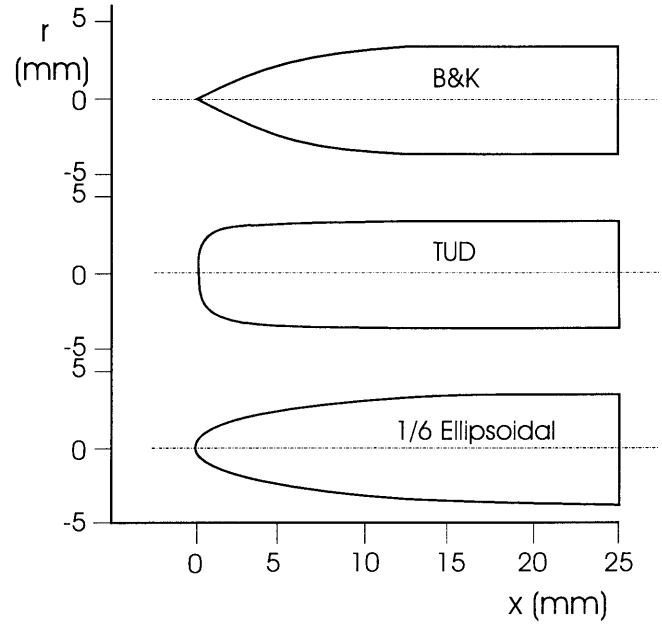

Fig.4: B&K, TUD and Ellipsoidal 1/4" AMF outer shapes

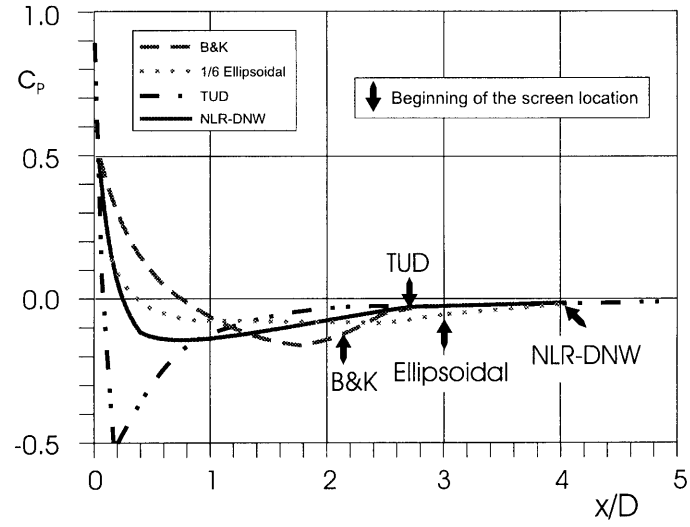

Fig.5: Envelope of pressure distributions along the axial co-ordinate of B&K, TUD, 1/6 Ellipsoidal and NLR-DNW AMF

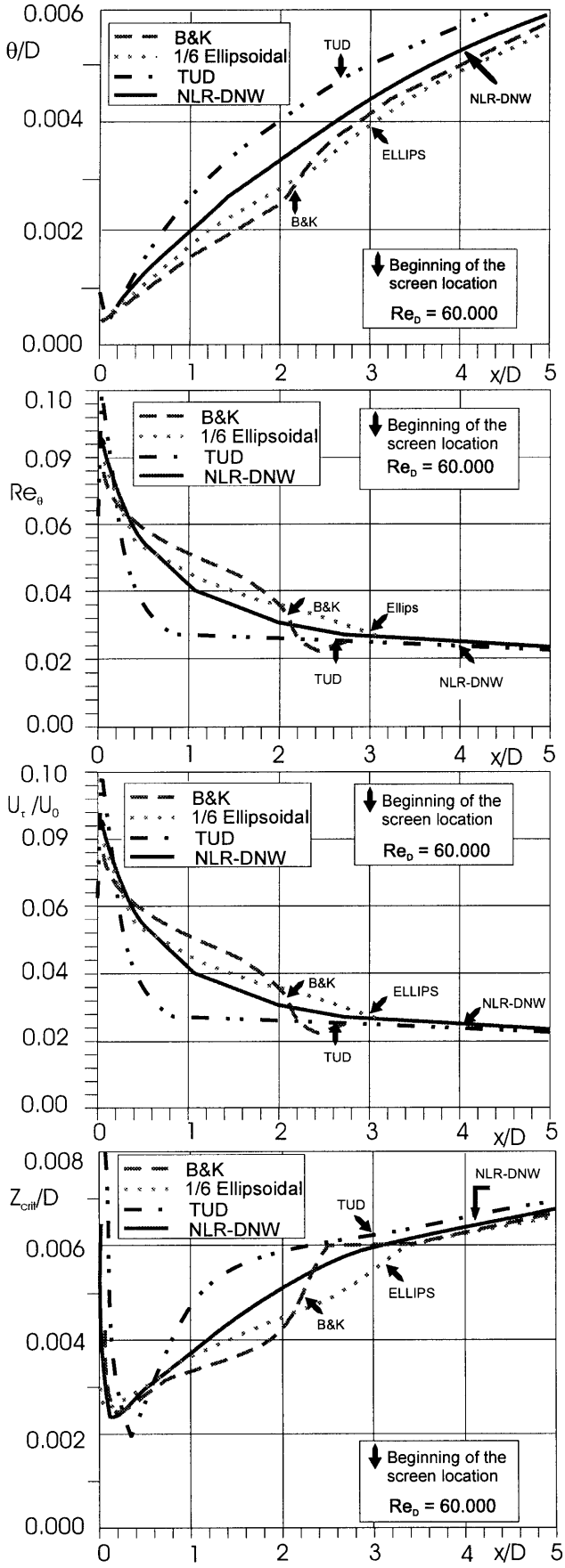

Fig.6a-d: Envelope of θ, Re_θ, U_τ and z_{crit} along the axial co-ordinate of B&K, TUD and Ellipsoidal AMF and NLR-DNW AMF

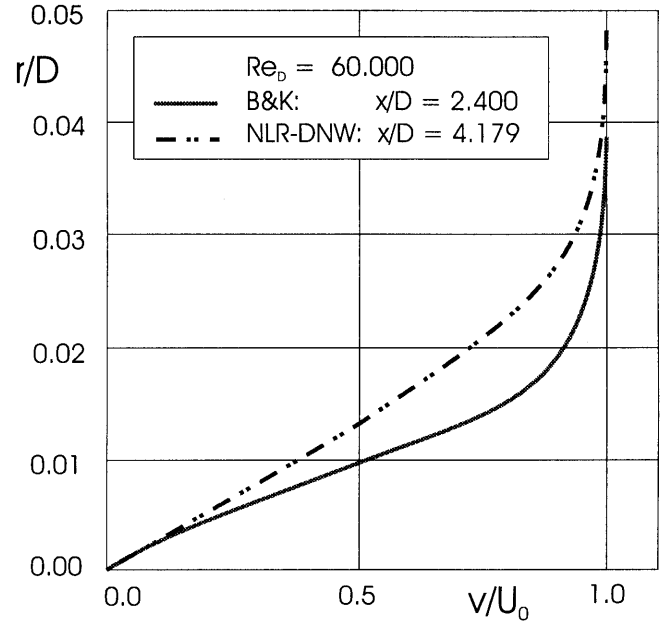

Fig.7: Boundary layer velocity profiles at screen positions of B&K AMF and NLR-DNW AMF

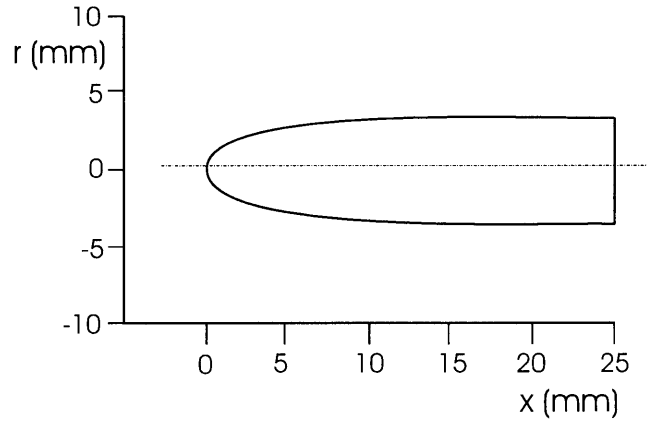

Fig.8: NLR-DNW AMF outer shape

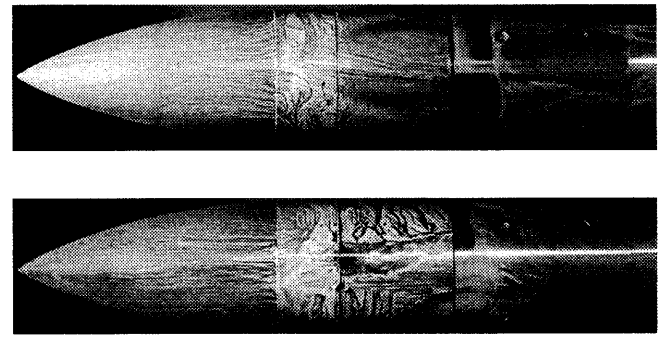

Fig.9: Picture of typical dye pattern at B&K AMF screen

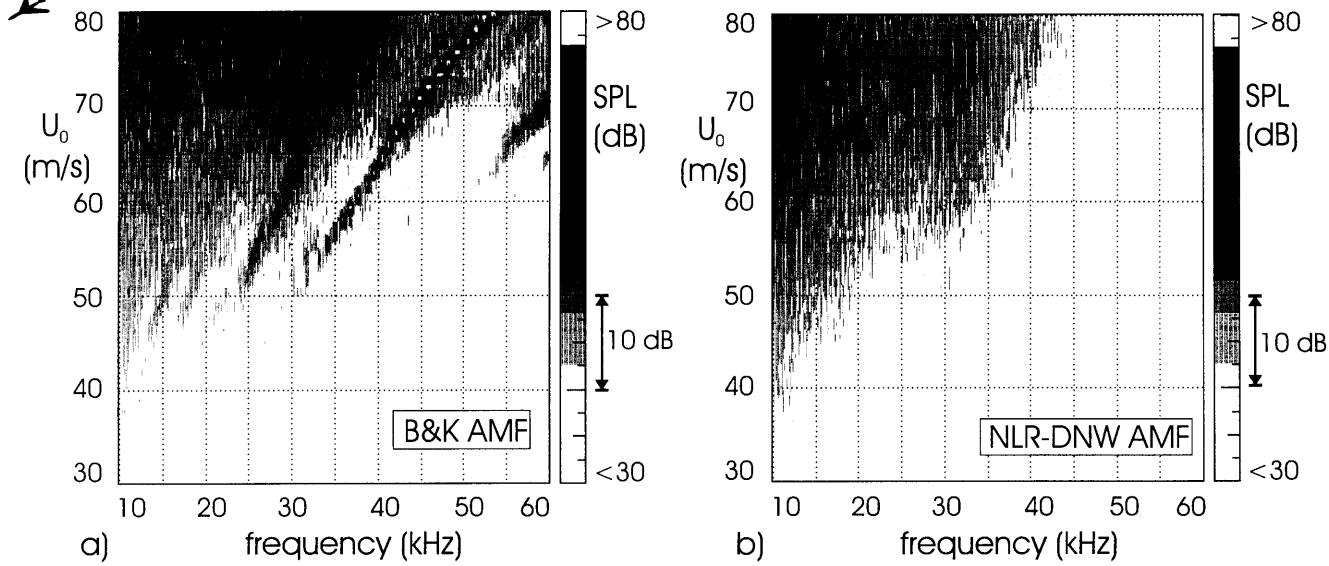

Fig.10a-b: Self-noise spectra of B&K (a) and NLR-DNW AMF (b) as a function of flow velocity

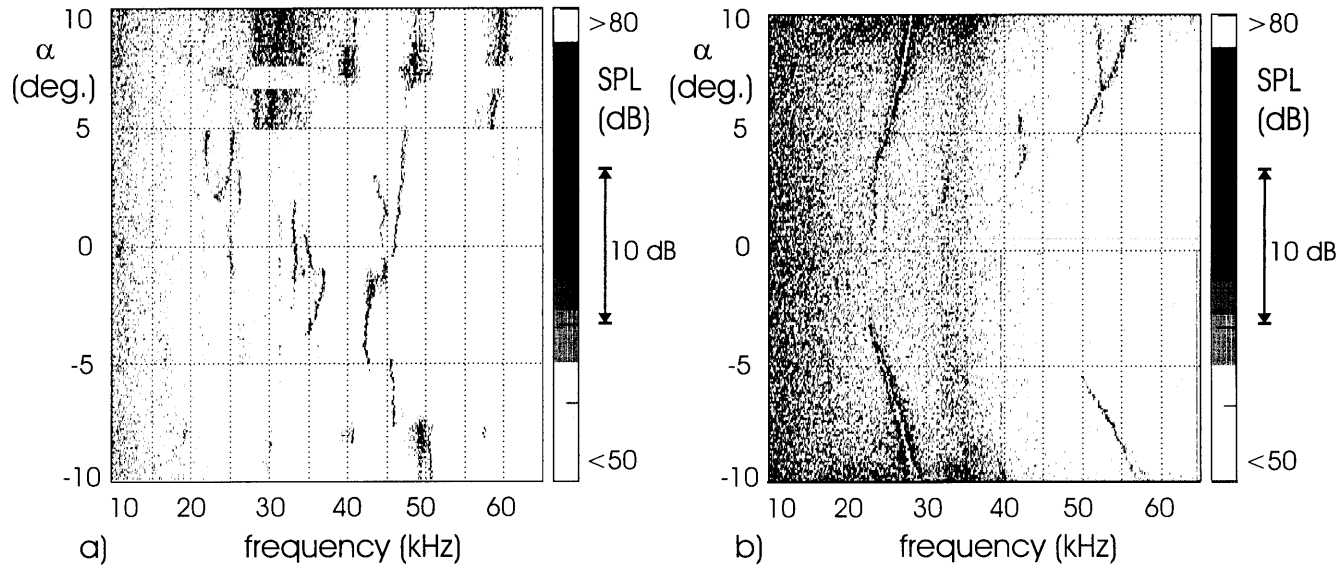

Fig.11a-b: Self-noise spectra of B&K (a) and NLR-DNW AMF (b) as a function of flow angle

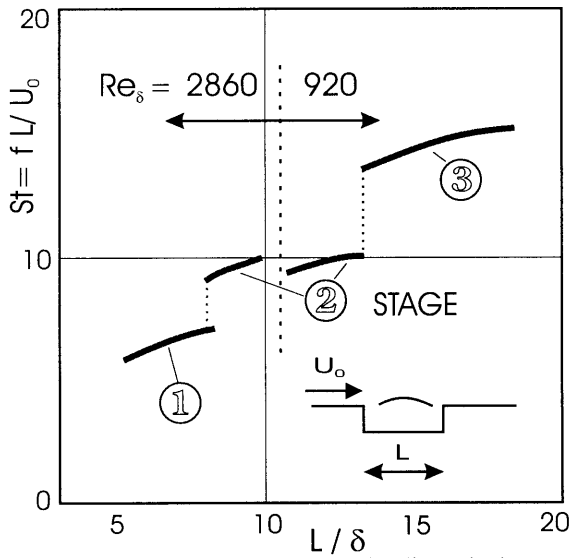

Fig.12: Variation of Strouhal number with dimensionless impingement distance for cavity oscillations (after Ref. 9)

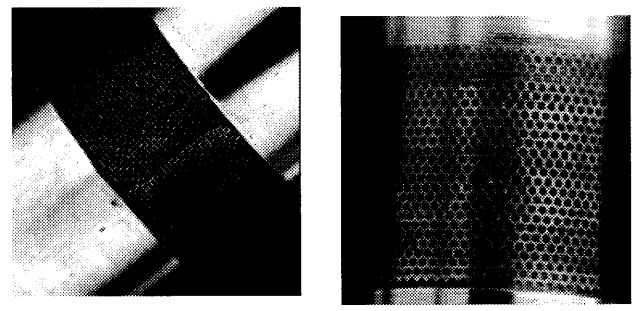

Fig.13: Pictures of B&K mesh and of PERFOLIN AMF screen

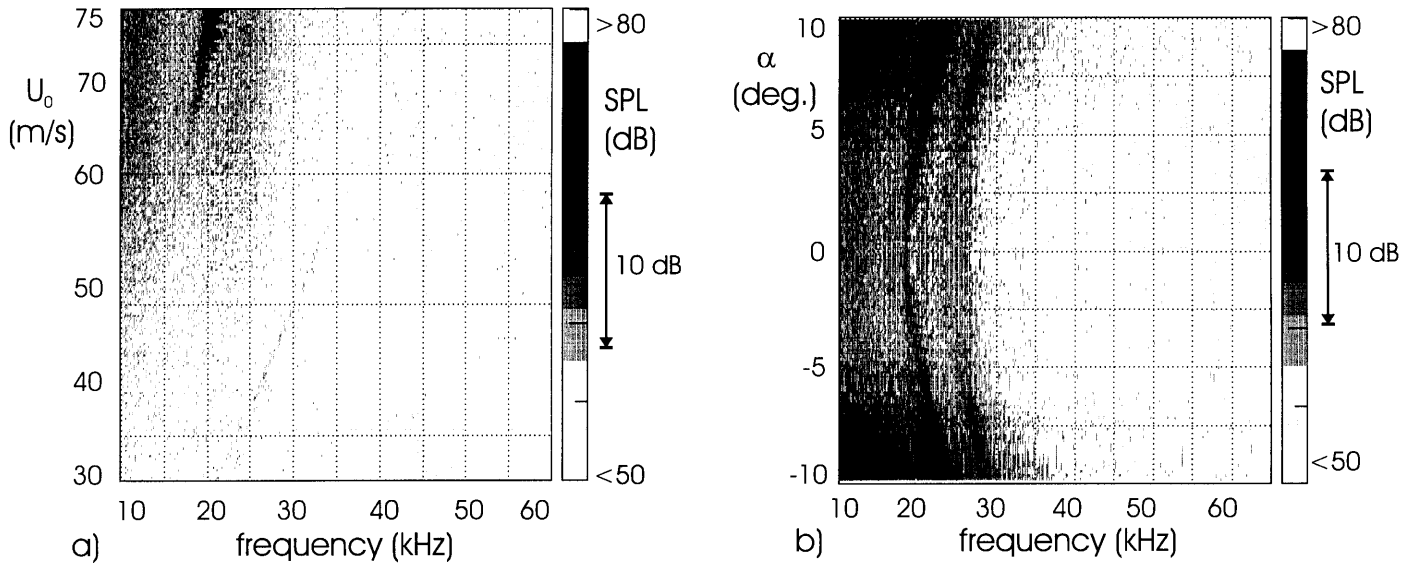

Fig.14: Self-noise spectra of modified NLR-DNW AMF (as measured in the NLR anechoic wind tunnel) as function of flow velocity U_0 (a) and angle of attack α (U_0= 70 m/s) (b)

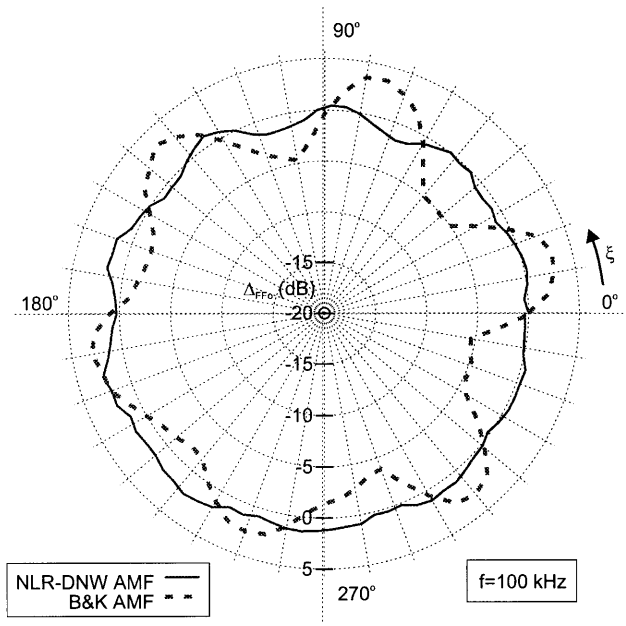

Fig.15: Azimuthal envelope of free-field correction for B&K 1/4" microphone equipped with B&K AMF and with modified NLR-DNW AMF (Θ=90°)

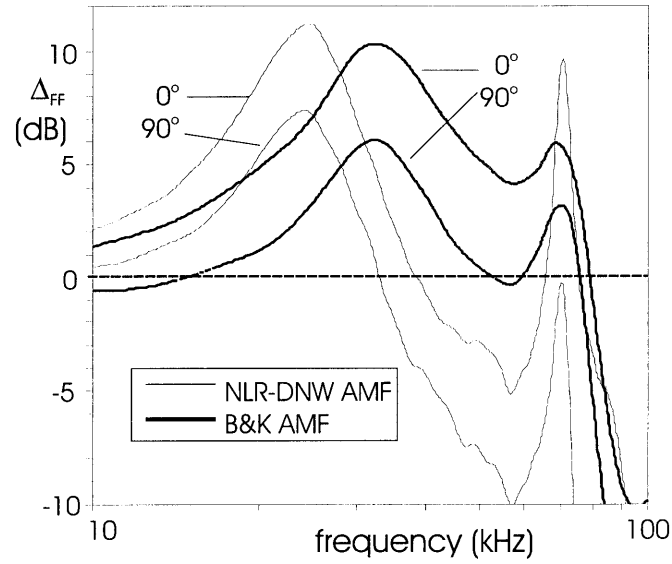

Fig.17: Free-field corrections for B&K 1/4" microphone equipped with B&K AMF and with modified NLR-DNW AMF for Θ=0°and Θ=90°

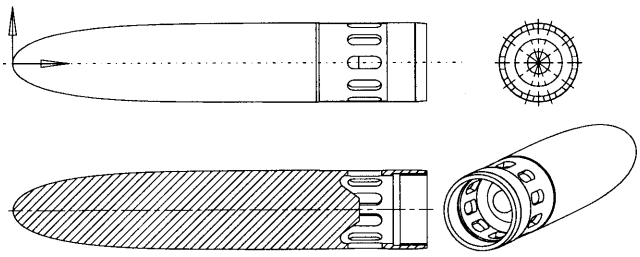

Fig.16: Modified NLR-DNW AMF outer shape, cross section and interior